Dalton Transactions

ROYAL SOCIETY OF CHEMISTRY

PAPER

View Article Online
View Journal | View Issue

Check for updates

Cite this: *Dalton Trans.*, 2025, **54**, 12180

Published on 21 Mawuwani 2025. Downloaded on 2025-12-11 12:58:38.

Complex of copper(II) hexafluoroacetylacetonate with photochromic spiropyran in the merocyanine form: field-induced slow magnetic relaxation and quantum coherence for Cu^{II} (S = 1/2) and photoswitching of spiropyran ligand†

Nikita G. Osipov,[a] Maxim A. Faraonov,[a] Ilya A. Yakushev,[b] Sergey L. Veber,[c,d] Matvey V. Fedin,[c,d] Nikolay N. Denisov,[a] Alexander F. Shestakov,[a] Akihiro Otsuka,[e] Hiroshi Kitagawa[e] and Dmitri V. Konarev*[a]

Received 14th May 2025,
Accepted 18th July 2025

DOI: 10.1039/d5dt01129a

rsc.li/dalton

The interaction of photochromic 8-methoxy-1′,3′,3′-trimethyl-6-nitro-spiro[chromene-2,2′-indole] (MNSP) spiropyran with copper(II) hexafluoroacetylacetonate yields a deep red–violet solution due to a coordination-induced transition of MNSP from its closed form to the colored, open merocyanine (MC) form. The crystal structure of {Cu^{II}(hfac)$_2$·MNSP} (**1**) shows coordination of two oxygen atoms in MNSP to Cu^{II}, forming a distorted octahedral geometry with four short (1.94–1.97 Å) and two longer (2.22–2.44 Å) Cu–O bonds. The $\chi_M T$ value of 0.43 emu K mol^{-1} at 300 K corresponds to a g-factor of 2.16 for Cu^{II} (S = 1/2). The electron paramagnetic resonance (EPR) signal fits well with $g_{\|}$ = 2.071, $g_{\perp}$ = 2.347 (g_{iso} = 2.167), and $A_{\perp}$ = 420 MHz. Slow magnetic relaxation is observed under a static magnetic field of 2000 Oe with χ'' (ν) curves showing well-defined maxima in the 2.0–6.0 K range. The dependence of ln(τ) *vs.* 1/T is well described using a linear combination of direct and Raman relaxation mechanisms. A magnetic hysteresis loop is observed at 0.5 K, classifying complex **1** as a single-ion magnet. This loop closes at zero field due to quantum tunneling of the magnetization but reopens at fields exceeding ±100 Oe. Pulsed EPR spectroscopy reveals quantum coherence with T_m ~ 0.3 μs at 10 K. The spin–lattice relaxation time, T_1 = 0.7 ms, correlates well with values obtained from AC susceptibility data. A blue shift of 40–60 nm in the main absorption band of the open MC form of MNSP is observed upon complex formation. The complex dissociates in dilute solutions but reforms reversibly under ultraviolet (UV) and green light excitation. It remains stable in concentrated solutions or films. In solution, green and UV light reversibly switch the ligand between the open and closed forms within the complex, whereas only partial switching is observed in films.

1. Introduction

Photochromic spiropyran molecules can reversibly switch between the closed spiropyran (SP) and open merocyanine (MC) forms in response to different stimuli.[1,2] The MC form exhibits an intense absorption in the visible range due to its nearly planar structure, enabling π-conjugation.[3] Therefore, the reversible SP–MC transformation alters the color of the compound and affects its properties.[1–3] External stimuli include light, temperature, solvent polarity, metal complexation, and others.[4,5] Photochromic molecules find applications in photoswitchable devices, energy acceptors, sensors, optical elements, and rewritable data storage devices.[6]

Spiropyrans contain oxygen atoms that, in the MC form, are available for coordination with metal ions (Scheme 1), forming

[a]*Federal Research Center of Problems of Chemical Physics and Medicinal Chemistry RAS, Chernogolovka, Moscow region, 142432 Russia. E-mail: konarev3@yandex.ru*
[b]*Kurnakov Institute of General and Inorganic Chemistry, RAS, Moscow, 119991 Russia*
[c]*International Tomography Center SB RAS, 630090 Novosibirsk, Russia*
[d]*Novosibirsk State University, 630090 Novosibirsk, Russia*
[e]*Division of Chemistry, Graduate School of Science, Kyoto University, Sakyo-ku, Kyoto 606-8502, Japan*

†Electronic supplementary information (ESI) available: Experimental, synthesis, X-ray diffraction data, IR, optical spectra of **1** and photoswitching, local symmetry of Cu^{II} in **1**, DC and AC measurements for **1**, CW EPR spectra, theoretical calculations for **1**. CCDC 2428887 and 2428888. For ESI and crystallographic data in CIF or other electronic format see DOI: **https://doi.org/10.1039/d5dt01129a**

This journal is © The Royal Society of Chemistry 2025

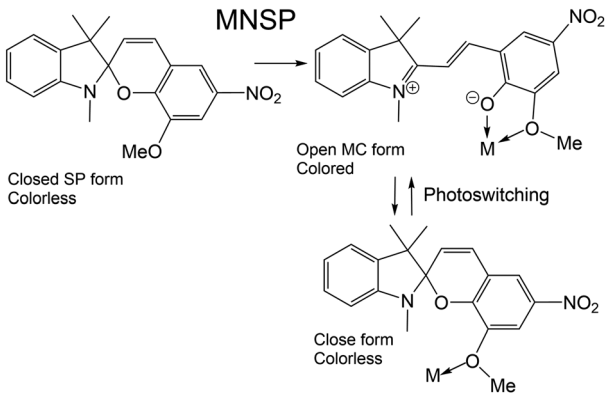

Scheme 1 Transition of photochromic 8-methoxy-1′,3′,3′-trimethyl-6-nitro-spiro[chromene-2,2′-indole] (MNSP) from its closed SP form to the open MC form upon coordination of its oxygen atoms to a metal center, and possible photoswitching of the ligand within the complex.

Published on 21 Mawuwani 2025. Downloaded on 2025-12-11 12:58:38.

coordination complexes. These were first described nearly 60 years ago by Philips and Taylor.[7] Spiropyrans can be photoresponsive even within several known complexes,[8] offering potential applications in the design of stimuli-responsive materials. Specifically, coordination assemblies of spiropyrans with paramagnetic metals are promising candidates for the design of photoswitchable magnetic materials. Among these, bistable magnets, whose properties can be influenced by light or other stimuli, are of particular interest; however, such assemblies are rare.

Recently, a dimeric complex of manganese(II) hexafluoroacetylacetonate $\{Mn^{II}(hfac)_2\}$ and $Fe^{III}X_3$ (X = Cl and Br) with the photochromic spiropyran ligand 1′,3′,3′-trimethylindolino-β-naphthopyrylospiran (TMI-NPS) was reported.[9] The spiropyran ligand coordinates with two Mn^{II} ions, inducing ferromagnetic coupling between them. Their spins align parallel to each other within the dimer, resulting in a high-spin $S = 5$ state at 2 K.[9a] Complexes of Dy and Yb with substituted spiropyrans were also developed. The Dy complex exhibited single-ion magnet (SIM) behavior with a magnetization reversal barrier (U_{eff}) of 150 cm^{-1}.[10] A complex of bidentate 8-methoxy-1′,3′,3′-trimethyl-6-nitro-spiro-[chromene-2,2′-indole] (MNSP) with $Co^{II}(hfac)_2$ was obtained which exhibited slow magnetic relaxation under a 1000 Oe external magnetic field.[11] Recently, SIMs were obtained through axial coordination of two TMI-NPS ligands to the Dy and Tb ions in $(TBA^+)\{(TMI\text{-}NPS)_2{\cdot}La^{III}I_4\}^-{\cdot}0.5C_6H_4Cl_2$. The Dy compound showed zero-field SIM properties up to 8 K with a high magnetization blocking barrier (U_{eff} = 470 cm^{-1}), whereas the Tb complex exhibited field-induced SIM properties under a 2000 Oe magnetic field.[12]

In addition to $Co^{II}(hfac)_2$,[11] coordination complexes of MNSP with $Sb^{III}Cl_3$, $Zn^{II}Cl_2{\cdot}EtOH$, and $ZnBr_2{\cdot}EtOH$ units were also synthesized and structurally characterized.[13] Studies showed that Cu^{II}, Zn^{II}, Ni^{II}, and La^{III} ions bind to two MNSP ligands, whereas Ca^{II} binds to four.[14,8c] Some of these complexes are photoresponsive.[8c] Therefore, we chose this spiropyran to prepare a potentially photoswitchable magnetic compound. Among various paramagnetic transition metals, copper (II) complexes are of particular interest for magnetic studies. Despite the lack of zero-field splitting in the Cu(II) ion (S = 1/2), slow magnetic relaxation under an applied DC field has been observed in its complexes.[15] An especially promising application involves the use of Cu^{II} ions as molecular spin qubits owing to their stable spin coherence.[16] The MNSP spiropyran (Scheme 1) in its MC form contains two oxygen atoms available for coordination, allowing MNSP to coordinate to $Cu^{II}(hfac)$, forming an octahedral Cu^{II} environment. The interaction of MNSP with $Cu^{II}(hfac)_2$ turns the toluene solution deep red–violet, indicating a coordination-induced transition of the spiropyran from the closed SP form to the open MC form. In this study, complex $Cu^{II}(hfac)_2{\cdot}$MNSP (**1**) was obtained as high-quality single crystals, and its structure along with its optical and magnetic properties were studied. The complex exhibits field-induced slow magnetic relaxation and displays even hysteresis loops at 0.5 K, qualifying it as a Cu-containing field-induced SIM. Although several Cu^{II} complexes with field-induced slow magnetic relaxation have been reported,[15] complex **1** represents the first such system with a photochromic ligand which can display magnetic hysteresis as well. Spin coherence on Cu^{II} nuclei was also demonstrated in **1**. Complete switching from the closed SP form to the open MC form occurs under UV light excitation of the solution, whereas green light completely switches MNSP ligand back to the closed SP form within the complex. In films, however, only partial switching is achieved. Thus, this magnetically active compound shows photoresponsive behavior at least in solution.

2. Results and discussion

a. Synthesis

Mixing $Cu^{II}(hfac)_2$ and MNSP in either *o*-dichlorobenzene or toluene yields a red–violet solution over 24 h, indicating the formation of the open MC form of MNSP due to coordination of both oxygen atoms (Scheme 1) to $Cu^{II}(hfac)_2$. Better crystals are obtained from toluene than from *o*-dichlorobenzene. Precipitation of crystals from dilute toluene solutions by *n*-hexane yields two phases: very thin red needles and large, red–violet dark prisms. Both types of crystals contain $Cu^{II}(hfac)_2{\cdot}$MNSP; however, the crystal structure of the red needles could not be determined with good precision due to their very small size. Consequently, only unit cell parameters are provided for these crystals in the Experimental section. By contrast, the crystal structure of the red–violet dark prisms was determined with good precision. A similar synthesis performed in a concentrated $Cu^{II}(hfac)_2$–MNSP solution (with toluene volume reduced fourfold) yielded only large dark red–violet prisms with a good yield (64%) and no admixtures. Therefore, we studied the properties of $Cu^{II}(hfac)_2{\cdot}$MNSP (**1**) phase prepared in its pure form. Elemental analysis was carried out to determine the obtained composition. Although

Published on 21 Mawuwani 2025. Downloaded on 2025-12-11 12:58:38.

the synthesis was conducted under anaerobic conditions, complex **1** is stable in air as a crystalline solid, film, or concentrated solution.

b. Optical stpectra

The starting MNSP is nearly transparent in the closed SP form. However, during the KBr pellet preparation under pressure, the obtained pellet turns blue, indicating partial formation of the open MC form. Therefore, the spectrum of MNSP in the KBr pellet contains bands attibutable to both the closed and open forms of the ligand.

Initially we studied the absorption spectra of starting MNSP in toluene solution (5.91×10^{-5} M) before and after UV-light (366 nm) photoexcitation. The initial solution is transparent, indicating that the open MC form does not form in low-polarity toluene. A brief UV excitation (15 seconds) turns the solution blue, and a new intense band appears in the spectrum at 603 nm (Fig. S3†), attributed to the photoinduced open MC form of MNSP. As previously discussed, the open form of MNSP can also form under pressure during KBr pellet preparation where the lowest-energy absorption band is at 557 nm. Thus, the open MC form of MNSP exhibits different position of lowest-energy absorption bands in solution and solid state with a 46 nm blue shift observed for the spectrum measured in KBr pellet.

Complex **1** in a KBr pellet shows an intense red–violet color with a lowest-energy absorption band at 518 nm. The non-coordinated open MNSP (formed under pressure in KBr pellet) exhibits this band at 557 nm; threfore, complex formation induces a 39 nm blue shift in this band (Fig. 1a). No distinct near-infrared (NIR) bands appear in the complex **1** spectrum, but the absorption decreases to zero only below 1500 nm (Fig. S2b†), indicating weak broad absorption bands between 900 and 1300 nm, supported by density functional theory (DFT) calculations (Table S3†). The starting $Cu^{II}(hfac)_2$ shows absorption bands at 227 and 312 nm (Fig. S2a†) and does not contribute to the visible-range absorption in complex **1**.

Complex **1** in toluene solution exhibits an unusual behavior. To obtain a qualitative spectrum, the starting solution of complex **1** was diluted ~100-fold, yielding a low-concentration solution of this complex (5.91×10^{-5} M). However, under these conditions, the solution decolorizes within minutes, indicating dissociation of the complex. Interestingly, immediately after dilution, the solution turns blue, indicating the formation of the open MC form of non-coordinated MNSP, after which the solution color slowly disappears. Therefore, a qualitative spectrum of complex **1** cannot be obtained at low concentration. Increasing the concentration 50-fold stabilizes the complex in solution for a long time. The coordinated and non-coordinated MNSP in the open form exhibit different lowest-energy absorption bands at 547 and 603 nm, respectively, indicating a 56 nm blue shift upon complex formation. This difference clearly reveals the open form of the ligand in its non-coordinated state which may appear under photoexcitation. We therefore conclude that this form is not produced in the presence of $Cu^{II}(hfac)_2$ as evidenced by the absence of the band at 603 nm (Fig. S4†).

The first experiment was conducted using a low-concentrated solution (5.91×10^{-5} M) (Fig. S4†). Initially, the complex is absent. Upon 15 s of UV light excitation the solution turns red–violet, indicating complex formation, and a new absorption band appears at 547 nm. This band gradually decreases in intensity over 12 min, signaling dissociation of the complex. Extending UV exposure to 30 s enhances the transformation and prolongs the dissociation of the complex to 15 min. This switching is completely reversible and can be repeated multiple times.

The ligand-state switching within the complex was also studied in a more concentrated solution (8.87×10^{-5} M). At this concentration, the complex does not completely dissociate and remains partially stable for a long time (starting curve in Fig. 1b). UV irradiation (366 nm) within 30 seconds increases the intensity of the 547 nm band, indicating the photoinduced complex formation. Subsequent exposure to green light (548 nm) decolorizes the solution within 15 min, suggesting complete switching of the ligand to the closed SP form. Although dissociation of the complex may contribute to this process, the spectrum of the starting solution (Fig. 1b) shows

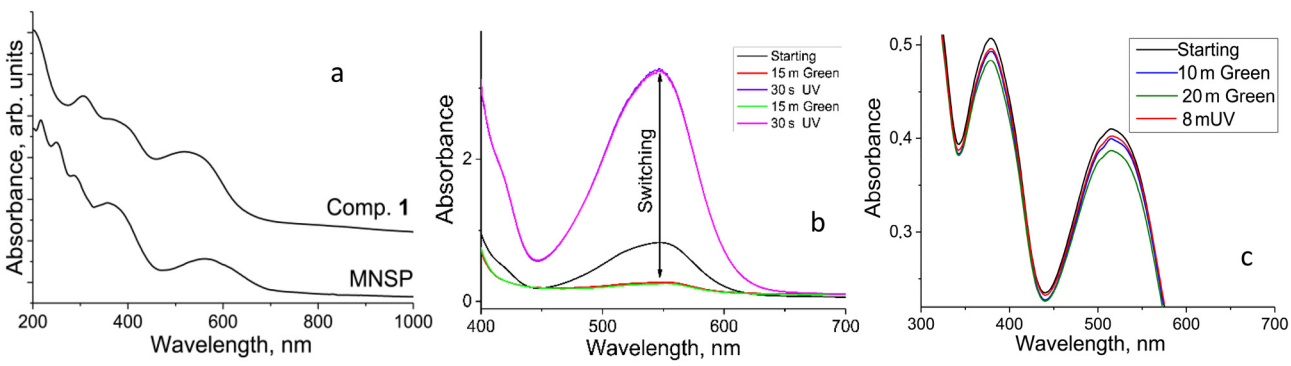

Fig. 1 (a) Spectra of starting MNSP and complex **1** in KBr pellets prepared under anaerobic conditions; (b) complete photoswitching of the ligand in the complex under the UV and green light excitation in toluene solution (concentration = 8.87×10^{-5} M); (c) partial photoswitching of the ligand in the film of $Cu^{II}(hfac)_2$·MNSP complex under green and UV light excitation in aerobic conditions (only part of the spectrum is shown).

 This journal is © The Royal Society of Chemistry 2025

Published on 21 Mawuwani 2025. Downloaded on 2025-12-11 12:58:38.

that the dissociation is incomplete under these conditions. This completely reversible switching can be repeated many times; two representative cycles are shown in Fig. 1b.

Complex **1** remains stable in film for a long time even under air. Green light excitation partially decreases the intensity of the band associated with the open MNSP in the complex with the switching degree increasing with exposure time (compare 10 and 20 min in Fig. 1c). However, prolonged exposure is needed for further reduction in the band intensity. A partial restoration of this band occurs after 8 min of UV light exposure. Similar behavior is observed under anaerobic conditions. Thus, contrary to the solution state, only partial switching of the ligand occurs in the film.

The infra-red spectrum of complex **1** is shown in Fig. S1† with peak positions listed in Table S1.† The spectrum represents a superposition of bands from MNSP and $Cu^{II}(hfac)_2$.

c. Crystal structure

The crystal structure of complex **1** was studied at 100 and 250 K (Fig. S5†). Although complex **1** is isostructural with the previously reported $Co^{II}(hfac)_2$·MNSP,[11] several notable differences are observed between the two. The $Co^{II}(hfac)_2$·MNSP complex undergoes a transition at 170 K with a 5.5% decrease in unit cell volume, affecting its magnetic properties.[11] In contrast, such transition is not observed for complex **1**; as temperature drops from 250 to 100 K, its unit cell volume decreases gradually by only 43 Å^3 (2.6%). The MNSP ligand coordinates through two oxygen atoms to $Cu^{II}(hfac)_2$ forming an octahedral coordination environment with six O atoms around Cu^{II} (Fig. 2). SHAPE analysis[17] suggests that an octahedral geometry best describes the Cu^{II} coordination environment (Table S2†). A similar, distorted octahedral environment is observed for Co^{II} in $Co^{II}(hfac)_2$·MNSP,[11] although the geometries for cobalt and copper coordination differ. In **1**, four oxygen atoms form four short Cu–O bonds (1.94–1.97 Å), resulting in square-planar geometry (Fig. 2b and c), while the other two Cu–O bonds are elongated to 2.220(2) and 2.436(2) Å at 250 K. These two oxygen atoms lie above and below the O_4 square plane, creating an axially elongated octahedral geometry. Upon cooling to 100 K, the short Cu–O bond lengths remain unaffected, while the longest Cu–O bond length is slightly shortened from 2.436(2) to 2.421(1) Å (Fig. 2b and c). The octahedrality slightly decreases at 100 K (Table S2†).[17] Interestingly, this geometry resembles that of previously studied $Cu^{II}(hfac)_2$ complexes with pentaheterocyclic triphenodioxazine and other related Cu^{II} complexes in which the Cu^{II} coordination environment is close to an axially elongated octahedron or square. Such complexes generally show field-induced slow magnetic relaxation (Table 1).[15]

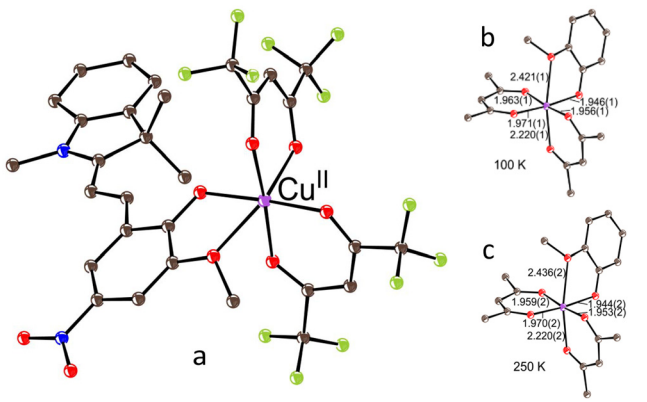

Fig. 2 Experimental crystal structure of **1**. (a) Visualization of the $Cu^{II}(hfac)_2$·MNSP unit in complex **1** at 100 K. Oxygen is red, fluorine is light green, carbon is brown, nitrogen is blue, and copper is violet. An Ortep drawing with equivalent isotropic atomic displacement parameters is shown. (b) and (c) Depiction of the distorted octahedral surrounding of Cu^{II} formed at the interaction with six oxygen atoms from hfac and MNSP at 100 and 250 K, respectively. The length of the Cu–O bonds is shown. Only PhO_2Me fragment of MNSP is depicted.

The $Cu^{II}(hfac)_2$·MNSP units form chains along the *a* axis where the NO_2 acceptor group of one ligand is positioned above the phenyl ring of MNSP from the neighboring $Cu^{II}(hfac)_2$·MNSP unit, with N···C and O···C contacts in the 3.24–3.26 Å range at 100 K (Fig. S6†). The shortest Cu···Cu distance is observed between the adjacent chains (7.50 Å), while the Cu···Cu distance within the chains is 10.88 Å. Both these distances are rather long, indicating the possibility of only weak intermolecular Cu···Cu coupling in this complex.

Upon green-light irradiation, the excitation of the $Cu^{II}(hfac)_2$·MNSP complex switches MNSP ligand from the open MC form to the closed SP form. To elucidate the structure of this complex in the excited state, DFT calculations were carried out (Fig. 3).[18] In the excited state, only one oxygen atom of the OMe group in MNSP remains available for coordination. This bond is elongated from 2.42–2.44 Å (experimental data at 100 and 250 K) to 2.69 Å (excited state). Therefore, the energy of its formation is much lower than that of the $Cu^{II}(hfac)_2$ complex with the open MC form of MNSP (see further discussion in the Theoretical section).

d. Magnetic properties of complex 1

The $\chi_M T$ value for complex **1** at 300 K is 0.43 emu K mol^{-1} (Fig. 4a) which is close to the spin-only value of 0.375 emu K mol^{-1} for a system with one independent $S = 1/2$ spin at $g = 2$. The $\chi_M T$ value remains constant upon cooling down to 5 K

Table 1 Optical spectral data of starting MNSP and its complex with $Cu^{II}(hfac)_2$ in toluene solution and KBr pellet

Compound and state	Absorption bands in the UV-optical and NIR range, nm
MNSP	
Solution, closed	355
Solution, open (excited)	289, 365, 603
KBr pellet	214, 248, 284, 356, 557
(**1**)	
Solution	303, 372, 547
KBr pellet	303, 357, 518

NIR: near infra-red; UV: ultraviolet.

Published on 21 Mawuwani 2025. Downloaded on 2025-12-11 12:58:38.

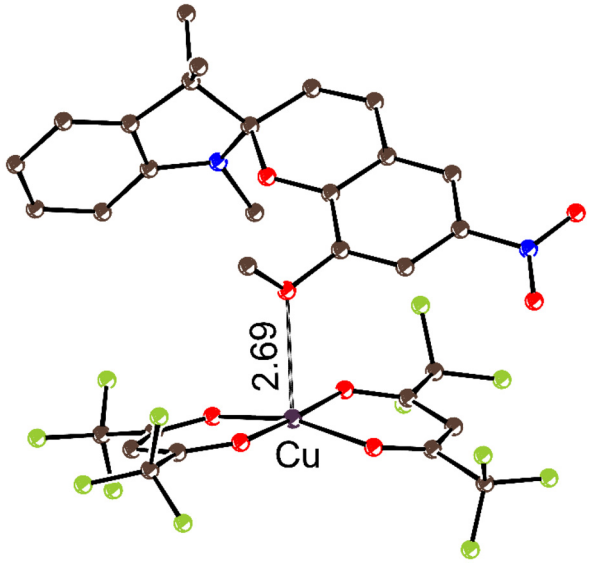

Fig. 3 Molecular structure of the $Cu^{II}(hfac)_2$·MNSP complex with the closed MNSP form based on DFT calculations.

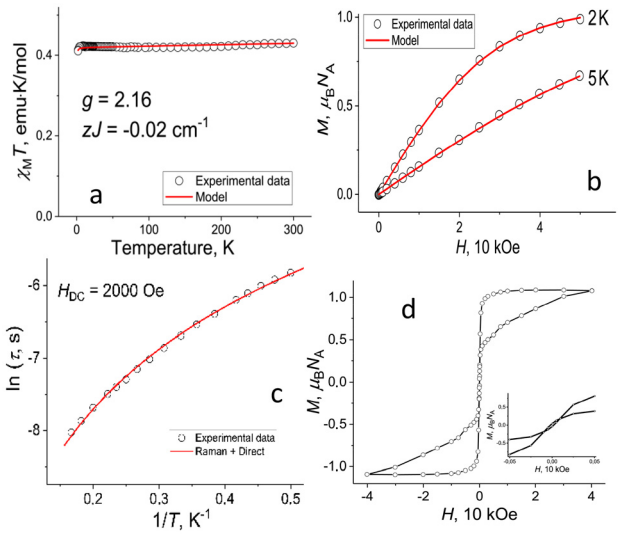

Fig. 4 (a) Temperature-dependent $\chi_M T$ values measured at H = 1 kOe and (b) field-dependent magnetization for complex **1** at 2 and 5 K. Experimental data are shown as open circles, with data fitting (with PHI program)[19] represented by solid red curves; (c) dependence of relaxation times ln(τ) on reciprocal temperature for complex **1** under H_{DC} = 2000 Oe. The solid red line represents the Arrhenius approximation based on the sum of the direct and Raman relaxation mechanisms; (d) hysteresis loops for polycrystalline complex **1** at 0.5 K with the inset picture exhibiting an expanded view of the variable-field magnetization near zero field.

below which a slight decrease in $\chi_M T$ value is observed. This decrease is likely due to weak intermolecular antiferromagnetic coupling between Cu^{II} spins. A simultaneous fit was carried out for the temperature dependence of $\chi_M T$ (Fig. 4a) and the magnetization *versus* the magnetic field at 2 and 5 K (Fig. 4b) by using the PHI program.[19] Hamiltonian used for these calculations is provided in the ESI.† Anisotropic g-factor values were derived from fitting the electron paramagnetic resonance (EPR) spectrum of polycrystalline complex **1** measured at 4.2 K (Fig. 5a). This spectrum was well fitted using the EasySpin program[20] with the following parameters: $g_{\parallel}$ = 2.071, $g_{\perp}$ = 2.347 (g_{iso} = 2.167), and $A_{\perp}$ = 420 MHz (Fig. 5a). Notably, the same signal parameters were observed in both 0.1 and 1 mM glassy solutions of complex **1** (Fig. S12†), whereas the EPR spectrum of pure $Cu^{II}(hfac)_2$ exhibits essentially different parameters (Fig. S13†). Such g-factors have previously been reported for different Cu^{II} complexes showing field-induced slow magnetic relaxation (Table 2) and are indicative of easy-axis-type magnetic anisotropy, a feature typical of such complexes. Consequently, an isotropic g-factor of 2.16 and a small antiferromagnetic intermolecular exchange interaction parameter (zJ) of −0.02 cm^{-1} were obtained for **1** (Fig. 4a). The EPR data support the Cu^{II} g-factor values derived from SQUID analysis. This antiferromagnetic coupling most likely occurs along the chains (Fig. S6†) containing the MNSP ligands because weak π–π stacking and short intermolecular contacts are present between the MNSP ligands despite the shorter Cu···Cu distance of 7.50 Å between adjacent chains. This weak antiferromagnetic coupling is further supported by the small negative Weiss temperature of −2 K (Fig. S8†). The magnetization of complex **1** does not saturate up to an applied magnetic field of 50 kOe at 2 and 5 K, reaching values of 0.98 and 0.65$\mu_B N_A$, respectively (Fig. 4b).

Dynamic magnetic susceptibility measurements were carried out for complex **1**. AC measurements at applied external DC fields up to 5000 Oe (Fig. S10†) revealed intensive out-of-phase signals in the $\chi''(\nu)$ curves with the optimal DC field determined to be 2000 Oe (Fig. S10b†), indicating slow magnetic relaxation under the applied static magnetic field. At 2000 Oe, the $\chi''(\nu)$ curves recorded over the frequency range of 10–1500 Hz exhibit well-defined maxima between 2.0 and 6.0 K (Fig. S11b†). The resulting plot of ln(τ) as a function of inverse temperature for the relaxation process is shown in Fig. 4c. The experimental data were fitted well using eqn (1) which is a linear combination of the direct and Raman mecha-

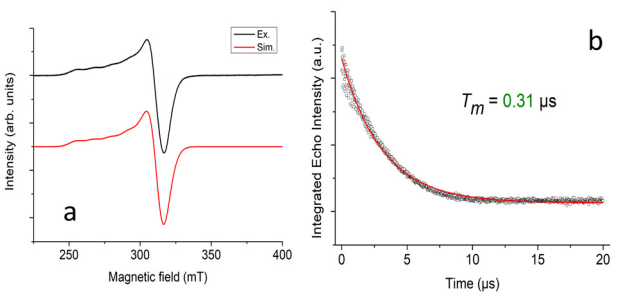

Fig. 5 (a) EPR spectrum of complex **1** measured at 4.2 K, with spectrum fitting performed using EasySpin software.[20] Fitting parameters are shown in the main text; (b) pulsed EPR ED traces for a 0.1 mM glassy solution of complex **1** at 10 K (black: experimental, red: fitting).

This journal is © The Royal Society of Chemistry 2025

Published on 21 Mawuwani 2025. Downloaded on 2025-12-11 12:58:38.

Table 2 Magnetic data for the Cu^{II} complexes showing field-induced slow magnetic relaxation

Compound	Coordination environment	EPR $g_{\parallel}$, $g_{\perp}$	Relaxation mechanisms and parameters	Ref.
[Cu(pydca)(dmpy)]·0.5H_2O	O_4N_2, axially elongated octahedron	2.051, 2.385	Raman + direct + QTM C_1 = 4.3(2) × 10^{-3} s^{-1} K^{-n}, n = 5 (fixed) C_2 = 5.2(4) × 10^3 s^{-1} K^{-1}, H_{DC} = 0.5 T	15*a*
[Cu(12-TMC)Cl][BPh_4]	N_4Cl, square pyramid	2.07, 2.22	Raman + direct + QTM C_1 = 8.31(3) s^{-1} K^{-n}, n = 3.10(2) C_2 = 1838.51(9) s^{-1} K^{-1}, H_{DC} = 0.15 T	15*b*
2[$Cu(H_4TCPP)$]·4.5DMF·1.5H_2O [{CuTCPP}$Zn_2(H_2O)_2$]·2DMF	N_4, square	2.065, 2.2	Raman + direct n = 1.4–1.7 for H_{DC} = 0.1–0.3 T n = 0.7 for H_{DC} = 0.5 T	15*c*
[$Cu(hfac)_2$(ClTDPO)]$_n$	O_4N_2, axially elongated octahedron	2.064, 2.333	Raman + direct C_1 = 52.1(8) s^{-1} K^{-n}, n = 2.11(7) C_2 = 8.5(5) × 10^{-5} s^{-1} K^{-1}, H_{DC} = 0.05 T	15*d*
$Cu^{II}(hfac)_2$·MNSP	O_6, axially elongated octahedron	2.071, 2.347	Raman + direct C_1 = 83.1 ± 3.5 K^{-n} s^{-1}, n = 2.04 ± 0.03 C_2 = 0.92 ± 0.05 K^{-1} s^{-1}, H_{DC} = 0.20 T	This work

pydca: pyridine-2,6-dicarboxylato; dmpy: 2,6-dimethanolpyridine; 12-TMC: 1,4,7,10-tetramethyl-1,4,7,10-tetraazacyclododecane; TCPP: 5,10,15,20-tetrakis(4-carboxy-phenyl)porphyrin; ClTDPO: 2,4-di-(*tert*-butyl)-9-chlorobenzo[5,6][1,4]oxazine[2,3-*b*]-phenoxazine; QTM: quantum tunneling of the magnetization.

nisms. The fitting parameters for complex **1** are C_1 = 83.1 ± 3.5 K^{-n} s^{-1}, n = 2.04 ± 0.03, and C_2 = 0.92 ± 0.05 K^{-1} s^{-1}.

$$\tau^{-1} = C_1 T^n + C_2 T \text{ (Raman + direct)} \quad (1)$$

Magnetic hysteresis loops for complex **1** were measured at 0.5 (Fig. 4d), 2, and 5 K (Fig. S9†). At 2 K, this loop slightly opens for fields above ±3000 Oe (Fig. S9a†), but it is closed at 5 K (Fig. S9b†). At 0.5 K, the loop widens but remains closed in the zero-field region and opens at fields above ±100 Oe (Fig. 4d, inset). The butterfly-shaped hysteresis loops are characteristic of field-induced SIMs exhibiting efficient quantum tunneling of the magnetization (QTM) at zero field.[21] Moreover, the magnetization at 0.5 K rapidly saturates even at 1000 Oe magnetic field, approaching the maximum value (Fig. 4d).

Table 2 lists Cu^{II} complexes that are reported to exhibit field-induced slow magnetic relaxation. In these complexes, the direct and Raman processes mainly contribute to the relaxation. Notably, anomalously low Raman (T^n) exponent values in the range 0.7–3.1 have been reported (except for [Cu(pydca)(dmpy)]·0.5H_2O, where n was fixed at 5) (Table 2). Theoretically, n values at low temperatures are expected to be between 5 and 9.[22] Recent theoretical investigations[23] have aimed to elucidate the physical reasons for such low n values. One possible explanation of low n values is the phonon bottleneck effect which depends on the concentration of magnetic ions and frequently leads to a $\tau^{-1} \sim T^2$ dependence at high ion concentrations. In this study, the obtained value of n is 2.04 ± 0.03 which is close to 2.0.

The observation of slow magnetic relaxation in complex **1** indicates a relatively long spin–lattice relaxation time up to 1 ms (Fig. 4c), suggesting a comparatively long decoherence time. The corresponding parameters were obtained using the pulsed EPR technique. A two-pulse echo-detected (ED) EPR spectrum was recorded for a frozen (glassy) 0.1 mM solution of complex **1** (Fig. S14†). The obtained ED spectrum was well simulated using previously determined parameters: $g_{\parallel}$ = 2.071, $g_{\perp}$ = 2.347, and $A_{\perp}$ = 420 MHz. Pulsed EPR Hahn echo decay traces for the solution at 336.4 mT were then acquired at 10 K, yielding a coherence time (T_m) of 0.31 μs (Fig. 5b). The spin–lattice relaxation time (T_1) of ∼0.7 ms was determined using the inversion recovery method (Fig. S15†). Notably, this value correlates well with the corresponding time (up to 1 ms) determined from the AC measurements. Spin–lattice (T_1) and spin–spin (T_m) relaxation times were derived by fitting the experimental curves using the exponential eqn (2):

$$I = I_0 + A \exp(-\tau/T_{m,1}). \quad (2)$$

e. Theoretical section

Experimental data show that the complex of MNSP with $Cu^{II}(hfac)_2$ is unstable at low concentrations. The dissociation of the complex into its initial components rapidly transfers MNSP from the blue open form to the colorless closed form. Quantum chemical modeling results for the transformation of the open to closed MNSP forms are shown in Fig. 6. This reaction occurs with an energy gain in two stages. The initial *trans*-configuration, in the first stage, transitions to the isomeric open *cis*-configuration in which the C and O atoms are in close proximity. In this configuration, only a small barrier must be overcome to form the C–O bond. The first step is the rate-determining stage with the semi-transformation time estimated as 27 min using the activated complex theory. This value is in reasonable agreement with the experimental time of 12–15 min, considering that the influence of solvent was not accounted for in the calculations. Due to steric constraints, only one oxygen atom of the methoxy group is available for coordination with $Cu^{II}(hfac)_2$ in the closed form. The formation energy of this complex (its structure shown in Fig. 3) is 10 kcal mol^{-1} lower than that of the chelate complex with the

Published on 21 Mawuwani 2025. Downloaded on 2025-12-11 12:58:38.

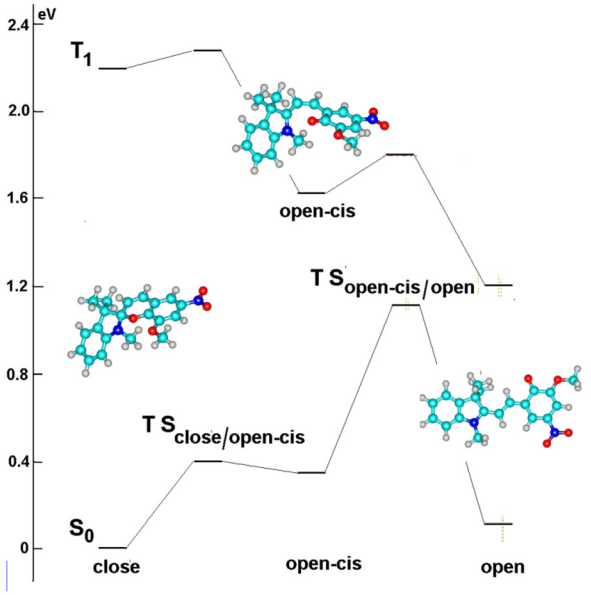

Fig. 6 Energetic diagram for the transformation of MNSP from closed to open form under UV light excitation and the reverse process.

open MNSP form which involves two coordination Cu–O bonds. Thus, the complex with the closed MNSP form is less stable than that with the open form, and it cannot form in low-concentrated solutions, where even the more stable open-form complex is prone to dissociation.

The instability constant in the gas-phase approximation is 10^{-2} mol L^{-1}. In solution, translational and rotational degrees of freedom are converted to librational modes which contribute less to the system entropy, making this value an upper limit. From experimental data, the constant is approximately 10^{-4} mol L^{-1}. Using this value and the calculated energy difference between the complexes of $Cu^{II}(hfac)_2$ with the open and closed forms of the ligand, the estimated instability constant of the complex with the closed form is approximately 2000 mol L^{-1}.

Nevertheless, after dissociation of the complex with open form of the ligand in the low-concentration solutions, it reforms upon photoexcitation. This can be explained by light-induced isomerization of the spiroform which temporarily enhances the binding strength of $Cu^{II}(hfac)_2$ compared to the ground-state open form.

After photoexcitation, the excited singlet state of the closed form of the ligand appears. Isomerization to the open form becomes feasible only after its relaxation to the excited triplet state which requires some time. The energy profile for the transformation of the lowest triplet state of the ligand is shown in Fig. 6. The transformation occurs rapidly due to the large energy gain and small energy barriers for this transformation. The essential spin density is localized on the C=C bond in the open *cis*-form accounting for the relatively small barrier to its isomerization into the *trans*-form. When the ligand in its triplet-state open form interacts with $Cu^{II}(hfac)_2$, a complex is formed in the quartet or excited doublet state. The structure of the quartet complex is shown in Fig. S16a.† The energy gain upon formation is 4.1 kcal mol^{-1} lower than that of the formation of the ground-state doublet complex, despite comparable Cu–O coordination bond lengths. An increase in interaction energy is expected for the antiparallel orientation of the ligand and Cu^{II} spins. In this case, a more tightly bound complex forms with a dissociation energy 2.8 kcal mol^{-1} higher than that of the ground-state doublet complex. Accordingly, its instability constant is over two orders of magnitude smaller.

The geometric parameters of the excited complexes in the quartet and doublet states are quite similar. Cu–O bonds with hfac ligands lengthened by an average of 0.05 Å, while the coordination bond with the O atom of the methoxy group shortened by 0.43 Å. The relaxation energy associated with these changes is small, around 1.7 kcal mol^{-1}. Thus, the most prominent decrease in the system energy occurs with antiferromagnetic spin ordering, while the subsequent shortening of the labile coordination bond with the methoxy group has a minimum effect.

These results qualitatively explain the temporary accumulation of the complexed open-form ligand upon irradiation of its low-concentration solution. Initially, the triplet-state open-form ligand forms a stable complex in the excited doublet state which decays upon relaxation to the ground state due to its high instability constant.

3. Conclusions

The complex $Cu^{II}(hfac)_2$·MNSP (**1**), consisting of the photochromic MNSP spiropyran and copper(II) hexafluoroacetylacetonate, was obtained in crystalline form. Spiropyran transitions to the open MC form, allowing coordination of two oxygen atoms of MNSP to Cu^{II}, yielding an elongated octahedral geometry around Cu^{II} formed by six oxygen atoms. Although five short Cu–O bonds can form, as observed in previously described $Co^{II}(hfac)_2$·MNSP,[11] the Cu^{II} centers in **1** prefer an elongated octahedral geometry, elongating one Cu–O bond with hfac. This geometry is characteristic of mononuclear Cu^{II} complexes showing field-induced slow magnetic relaxation.[15] Despite being well-known,[15] complex **1** is the first example of such a complex with a photochromic spiropyran ligand. Moreover, we showed for the first time the magnetic hysteresis exhibited by complex **1** at low temperatures, indicating that the complex is a real SIM. Previously, hysteresis had not been observed in Cu^{II} complexes showing field-induced slow magnetic relaxation.[15] Interestingly, complex **1** exhibits magnetic behavior even though only direct and Raman relaxation mechanisms are involved. Pulsed EPR spectroscopy showed a rather long quantum coherence ($T_m \sim 0.3$ μs). The spin–lattice relaxation time ($T_1 = 0.7$ ms) correlates well with the relaxation time determined from the AC measurements. Despite the presence of short Cu–O bonds, the complex has low formation energy and dissociates in low-concentrated solutions into the

 This journal is © The Royal Society of Chemistry 2025

Published on 21 Mawuwani 2025. Downloaded on 2025-12-11 12:58:38.

starting components. Photoexcitation of closed MNSP by UV light in the presence of $Cu^{II}(hfac)_2$ yields a complex that degrades slowly within 12–15 minutes. This rapid formation of the complex may occur through the *cis*-isomer of open MNSP. This form is generated under photoexcitation to the excited triplet state. This isomer has an essentially higher binding constant with $Cu^{II}(hfac)_2$ compared to the ground-state open form (as indicated by DFT calculations). The complex then relaxes to the ground state which is unstable and dissociates in low-concentration solutions. In high-concentration solutions, the complex is more stable. In this case, reversible transformation of the ligand from the closed to open form is possible within the complex upon green and UV light excitations, respectively. However, only partial switching of the ligand within the complex occurs in the film. Thus, the photoresponsive complex **1** with SIM properties at low temperatures was obtained. To observe photoswitching in the magnetic state of this complex, complete transformation of the ligand is needed in the film which was not achievable for this complex. The search for other complexes of this type is in progress.

Conflicts of interest

The authors declare that they have no competing interests.

Data availability

Experimental, synthesis, X-ray diffraction data, IR, optical spectra of **1** and photoswitching, local symmetry of Cu^{II} in **1**, DC and AC measurements for **1**, CW EPR spectra, theoretical calculations for **1**.

The data supporting this article have been included as part of the ESI.†

Crystallographic data for salt **1** has been deposited at the CCDC under 2428887 and 2428888 and can be obtained from CCDC.†

Acknowledgements

The preparation and study of complex **1** was supported by the Russian Science Foundation (project no. 24-13-00060). The infra-red absorption study was supported by the Ministry of Science and Higher Education of the Russian Federation (registration number 124013100858-3). Some magnetic measurements were supported by JSPS KAKENHI (Grant numbers JP20H05623 and JP23K23425). All quantum chemical calculations were performed using the computing capabilities of the Joint supercomputer center of the National Research Center "Kurchatov Institute". Pulsed EPR measurements were performed at the center of Collective Use "Mass Spetrometric investigations" SB RAS.

References

1 (*a*) Y. Hirshberg and E. Fischer, *J. Chem. Soc.*, 1954, 297–303; (*b*) V. I. Minkin, *Chem. Rev.*, 2004, **104**, 2751–2776; (*c*) V. I. Minkin, *Russ. Chem. Rev.*, 2013, **82**, 1–26.
2 G. Such, R. A. Evans, L. H. Yee and T. Davis, *J. Macromol. Sci., Part C*, 2003, **43**, 547–579.
3 R. Klajn, *Chem. Soc. Rev.*, 2014, **43**, 148–184.
4 M. Gehrtz, C. Bräuchle and J. Voitlaender, *J. Am. Chem. Soc.*, 1982, **104**, 2094–2101.
5 L. D. Weis, T. R. Evans and P. A. Leermakers, *J. Am. Chem. Soc.*, 1968, **90**, 6109–6118.
6 (*a*) J. Cusido, E. Deniz and F. M. Raymo, *Eur. J. Org. Chem.*, 2009, 2031–2045; (*b*) C. H. Li, Y. X. Zhang, J. M. Hu, J. J. Cheng and S. Y. Liu, *Angew. Chem., Int. Ed.*, 2010, **49**, 5120–5124, (*Angew. Chem.*, 2010, **122**, 5246–5250).
7 (*a*) J. P. Phillips, A. Mueller and F. Przystal, *J. Am. Chem. Soc.*, 1965, **87**, 4020; (*b*) L. D. Taylor, J. Nicholson and R. B. Davis, *Tetrahedron Lett.*, 1967, **8**, 1585–1588.
8 (*a*) J. D. Winkler, C. M. Bowen and V. Michelet, *J. Am. Chem. Soc.*, 1998, **120**, 3237–3242; (*b*) L. Evans, G. E. Collins, R. E. Shaffer, V. Michelet and J. D. Winkler, *Anal. Chem.*, 1999, **71**, 5322–5327; (*c*) G. E. Collins, L.-S. Choi, K. J. Ewing, V. Michelet, C. M. Bowen and J. D. Winkler, *Chem. Commun.*, 1999, 321–322; (*d*) T. J. Feuerstein, R. Müller, C. Barner-Kowollik and P. W. Roesky, *Inorg. Chem.*, 2019, **58**, 15479–15486.
9 (*a*) N. G. Osipov, M. A. Faraonov, A. F. Shestakov, M. V. Mikhailenko, A. V. Kuzmin, S. S. Khasanov, A. Otsuka, H. Yamochi, H. Kitagawa and D. V. Konarev, *New J. Chem.*, 2023, **47**, 5470–5476; (*b*) N. G. Osipov, M. A. Faraonov, A. V. Kuzmin, S. S. Khasanov, A. F. Shestakov, N. N. Denisov, T. A. Savinykh, A. Otsuka, H. Kitagawa and D. V. Konarev, *New J. Chem.*, 2024, **48**, 13526–13537.
10 (*a*) P. Selvanathan, G. Huang, T. Guizouarn, T. Roisnel, G. Fernandez-Garcia, F. Totti, B. Le Guennic, G. Calvez, K. Bernot, L. Norel and S. Rigaut, *Chem. – Eur. J.*, 2016, **22**, 15222–15226; (*b*) P. Selvanathan, V. Dorcet, T. Roisnel, K. Bernot, G. Huang, B. Le Guennic, L. Norel and S. Rigaut, *Dalton Trans.*, 2018, **47**, 4139–4148.
11 N. G. Osipov, M. A. Faraonov, I. A. Yakushev, N. N. Denisov, A. Otsuka, H. Kitagawa and D. V. Konarev, *Dalton Trans.*, 2024, **53**, 3159–3166.
12 N. G. Osipov, M. A. Faraonov, A. V. Kuzmin, S. S. Khasanov, A. A. Dmitriev, N. P. Gritsan, N. N. Denisov, A. Otsuka, H. Yamochi, H. Kitagawa and D. V. Konarev, *Inorg. Chem. Front.*, 2025, **12**, 2092–2102.
13 (*a*) E. A. Shilova, A. Samat and G. Pépe, *Z. Kristallogr.–New Cryst. Struct.*, 2011, **226**, 71–72; (*b*) V. K. Seiler, K. Robeyns, N. Tumanov, D. Cinčić, J. Wouters, B. Champagne and T. Leyssens, *CrystEngComm*, 2019, **21**, 4925–4933.
14 M. Baldrighi, G. Locatelli, J. Desper, C. B. Aakeröy and S. Giordani, *Chem. – Eur. J.*, 2016, **22**, 13976–13984.
15 (*a*) R. Boĉa, C. Rajnák, J. Titiŝs and D. Valigura, *Inorg. Chem.*, 2017, **56**, 1478–1482; (*b*) H.-H. Cui, W. Lv, W. Tong,

Published on 21 Mawuwani 2025. Downloaded on 2025-12-11 12:58:38.

X.-T. Chen and Z.-L. Xue, *Eur. J. Inorg. Chem.*, 2019, 4653–4659; (*c*) A. Urtizberea, E. Natividad, P. J. Alonso, M. A. Andres, I. Gascyn, M. Goldmann and O. Roubeau, *Adv. Funct. Mater.*, 2018, **28**, 1801695; (*d*) D. V. Korchagin, E. P. Ivakhnenko, O. P. Demidov, A. V. Akimov, R. B. Morgunov, A. G. Starikov, A. V. Palii, V. I. Minkin and S. M. Aldoshin, *New J. Chem.*, 2021, **45**, 21912–21918.

16 (*a*) M. Wakizaka, S. Gupta, Q. Wan, S. Takaishi, H. Noro, K. Sato and M. Yamashita, *Chem. – Eur. J.*, 2024, **30**, e202304202; (*b*) Y. Dai, Y. Fu, Z. Shi, X. Qin, S. Mu, Y. Wu, J.-H. Su, Y.-F. Deng, L. Qin, Y.-Q. Zhai, Y.-Z. Zheng, X. Rong and J. Du, *Chin. Phys. Lett.*, 2021, **38**, 030303; (*c*) M. Wakizaka and M. Yamashita, *Chem. Phys. Rev.*, 2025, **6**, 011301.

17 (*a*) M. Llunell, D. Casanova, J. Cirera, P. Alemany and S. Alvarez, Program SHAPE, University of Barcelona, Spain (version 2.1, March 2013). (*b*) M. Pinsky and D. Avnir, *Inorg. Chem.*, 1998, **37**, 5575–5582.

18 (*a*) J. P. Perdew, K. Burke and M. Ernzerhof, *Phys. Rev. Lett.*, 1996, **77**, 3865–3868; (*b*) D. N. Laikov, *Chem. Phys. Lett.*, 1997, **281**, 151–156.

19 N. F. Chilton, R. P. Anderson, L. D. Turner, A. Soncini and K. S. Murray, *J. Comput. Chem.*, 2013, **34**, 1164–1175.

20 S. Stoll and A. Schweiger, *J. Magn. Reson.*, 2006, **178**, 42–55.

21 (*a*) S. Jiang, B. Wang, G. Su, Z. Wang and S. Gao, *Angew. Chem., Int. Ed.*, 2010, **49**, 7448–7451; (*b*) J. P. Durrant, B. M. Day, J. Tang, A. Mansikkamäki and R. A. Layfield, *Angew. Chem.*, 2022, **134**, e202200525; (*c*) J. Emerson-King, G. K. Gransbury, G. F. S. Whitehead, I. J. Vitorica-Yrezabal, M. Rouzières, R. Clérac, N. F. Chilton and D. P. Mills, *J. Am. Chem. Soc.*, 2024, **146**, 3331–3342.

22 A. Abragam and B. Bleaney, *Electron Paramagnetic Resonance of Transition Ions*, University Press, Oxford, Oxford, 2012.

23 (*a*) A. Lunghi and S. Sanvito, *J. Phys. Chem. Lett.*, 2020, **11**, 6273–6278; (*b*) L. Gu and R. Wu, *Phys. Rev. B*, 2021, **103**, 014401.

This journal is © The Royal Society of Chemistry 2025